Exposure to Selenomethionine and Selenocystine Induces Redox-Mediated ER Stress in Normal Breast Epithelial MCF-10A Cells

Marc Dauplais, Stephane Romero, Myriam Lazard

Exposure to Selenomethionine and Selenocystine Induces Redox-Mediated ER Stress in Normal Breast Epithelial MCF-10A Cells

EXPOSURE TO SELENOMETHIONINE AND SELENOCYSTINE INDUCES REDOX-MEDIATED ER STRESS IN NORMAL BREAST EPITHELIAL MCF-10A CELLS

Marc Dauplais[1], Stephane Romero[1] and Myriam Lazard[1*]

[1]Laboratoire de Biologie Structurale de la Cellule, BIOC, École Polytechnique, CNRS-UMR7654, IP Paris, Palaiseau, France.

[*] Corresponding author: Myriam Lazard, Laboratoire de Biologie Structurale de la Cellule, BIOC, École Polytechnique, CNRS-UMR7654, IP Paris, Palaiseau, France
Email: myriam.lazard@polytechnique.edu
ORCID: 0000-0002-7154-1352

Acknowledgments: We thank Pierre Mahou and the Ecole Polytechnique Bioimaging Facility for imaging on their equipment partly supported by Agence Nationale de la Recherche (ANR-11-EQPX-0029 Morphoscope2, ANR-10-INBS-04 France BioImaging). We thank Jun Hoseki for sending the pIRES-puro3-ERroGFP-S4 plasmid and Nathalie Rocques for expert technical advice.

ABSTRACT

Selenium is an essential trace element co-translationnaly incorporated into selenoproteins with important biological functions. Health benefits have long been associated with selenium supplementation. However, cytotoxicity is observed upon excessive selenium intake. The aim of this study is to investigate the metabolic pathways underlying the response to the selenium-containing amino acids selenomethionine and selenocysteine in a normal human breast epithelial cell model. We show that both selenomethionine and selenocystine inhibit the proliferation of non-cancerous MCF-10A cells in the same concentration range as cancerous MCF-7 and Hela cells, which results in apoptotic cell death. Selenocystine exposure in MCF-10A cells caused a severe depletion of free low molecular weight thiols, which might explain the observed up-regulation of the expression of the oxidative stress pathway transcription factor NRF2. Both selenomethionine and selenocystine induced the expression of target genes of the unfolded protein response (GRP78, ATF4, CHOP). Using a redox-sensitive fluorescent probe targeted to the endoplasmic reticulum (ER), we show that both selenoamino acids shifted the ER redox balance towards an even more oxidizing environment. These results suggest that alteration of the redox state of the ER may disrupt protein folding and cause ER stress-induced apoptosis in MCF-10A cells exposed to selenoamino acids.

Keywords: selenomethionine, selenocystine, ER Stress, oxidative stress, MCF-10A, redox

INTRODUCTION

Selenium (Se) is an essential micronutrient for many living species, including humans. It is translationally incorporated as selenocysteine (SeCys) into a few proteins, some of which are antioxidant enzymes, protecting cells from harmful oxidative damage [1, 2]. Se deficiency has been associated with cardiomyopathy, increased risk of mortality, poor immune function and cognitive decline [3, 4]. In addition, several human studies have reported that selenium supplementation may attenuate the risk of developing cancer and other pathologies [5]. Thus, Se has become a widely used dietary supplement for humans and livestock [6, 7]. However, a recent systematic review of the literature indicate that no epidemiological evidence support a cancer-preventing effect of Se intake [8]. Despite its potential benefits, high levels of blood Se have been associated with an increased risk of developing certain types of cancer, hypertension, chronic diseases such as diabetes, and neurodegenerative diseases [9, 10] and the window between intakes that result in protection or toxicity is relatively narrow [11].

Toxicity is generally attributed to the ability of Se compounds to induce oxidative stress [12-14]. Pro-oxidant properties of Se originate from the in vivo conversion of Se-containing compounds into H_2Se or into selenols (RSeH) such as SeCys, methylselenol (MeSeH) or selenoglutathione (GSeH), which are readily oxidized by oxygen with concomitant generation of reactive oxygen species (ROS) [15, 16]. Redox cycling of selenols with glutathione (GSH) and oxygen or the thioredoxin/glutaredoxin (Trx/Grx) systems generates massive oxidative stress, which can damage nucleic acids, proteins and lipids and eventually lead to cell death due to apoptosis, necrosis or necroptosis [17, 18]. Additionally, redox-active Se compounds can alter the intracellular redox balance by oxidation of intracellular thiols or reaction with protein-thiol to form selenylsulfide or disulfide bridges between low molecular-weight thiols and proteins or between proteins, potentially leading to protein inactivation or aggregation [19-22].

Selenomethionine (SeMet), a non-redox active Se-containing amino acid, is the predominant form of Se in food products or supplements, accounting for more than 50% of human dietary selenium [23]. Although at higher concentrations than those observed for most redox-active Se compounds, SeMet displayed antiproliferative activity and cytotoxicity towards yeast as well as human cancer cells [24]. In human cancer cell lines, SeMet was shown to induce apoptosis, including activation of caspases and altered expression of pro-apoptosis proteins [25-28]. Misincorporation of SeMet in proteins might in principle generate toxicity. However, it has been shown in yeast and human cells that SeMet can support cell growth in the absence of methionine without significant toxicity [29, 30]. Therefore, SeMet toxic effects must be mediated by one or several of its metabolic products rather than by itself, although the precise mechanism remains to be deciphered.

Previous studies in our laboratory, using *Saccharomyces cerevisiae* as a model system, demonstrated that metabolization into redox-active selenohomocysteine and SeCys accounted for SeMet toxicity [31] in yeast. In particular, we showed that SeMet induced a proteotoxic stress caused by an accumulation of toxic protein aggregates that is dependent on metabolization of SeMet in SeCys. Misincorporation of SeCys, in the place of cysteine, in nascent polypeptide resulted in protein misfolding and aggregation, and upregulation of chaperones genes under the control of Heat Shock Factor 1 [32]. At present, the mechanisms and signaling pathways underlying SeMet mode of action as an antiproliferative agent in mammalian cancer cells are little understood. The mechanism evidenced in yeast may contribute to SeMet and SeCys toxicity in higher eukaryotes but remains to be addressed. To this end, we wished to perform a comparative analysis of SeMet and SeCys toxicity mechanisms in human cells. SeCys, being readily oxidized by oxygen, cannot be used directly. Selenocystine (SeCyt), which is efficiently reduced by intracellular GSH and disulfide reductases, was used as a precursor of SeCys.

In this study, we examined the signaling pathways activated by SeMet and SeCyt exposure on the non-cancerous breast epithelial MCF-10A cell line. We show that, in contrast to yeast, oxidative and ER stresses but not proteotoxic stress are involved in selenoamino acids cytotoxicity.

MATERIALS AND METHODS

Reagents, antibodies and plasmids

L-Selenomethionine (SeMet), L-methionine, D,L-selenocystine (SeCyt), L-cystine, DTT and Diamide were from Sigma.

The antibodies used were the anti-NRF2 [HL1021] (GTX635826), anti-HSP27 (GTX101145), anti-GRP78 (GTX127934), anti-ATF4 (GTX101943) rabbit antibodies from GenTex. The anti-CHOP mouse monoclonal antibody (66741-1-Ig) and anti-GAPDH mouse antibody (60004-1-Ig) were from Proteintech. Horseradish peroxidase-conjugated anti-mouse (GENA931) or anti-rabbit antibodies (A6154) were from Sigma.

The plasmid pIRES-puro3-ERroGFP-S4 was kindly provided by J.Hoseki (Kyoto University of Advanced Science, Kyoto, Japan) and is described in [33].

Cell culture

Hela and MCF-7 cells were grown at 37 °C in 5% CO_2 in RPMI 1640 + Glutamax medium (Gibco) with 10% FBS and 100 U/mL penicillin/streptomycin. The immortalized epithelial cell line from human breast MCF-10A was obtained from the Institut Curie collection of breast cell lines, organized and maintained by Thierry Dubois in Paris. MCF-10A cells were grown at 37 °C in 5% CO_2 in DMEM/F12 medium (Gibco) supplemented with 5% horse serum, 20 ng/mL epidermal growth factor, 10 µg/mL insulin, 100 ng/mL cholera toxin, 500 ng/mL hydrocortisone, and 100 U/mL penicillin/streptomycin. MCF-10A cells stably expressing roGFP-S4 were grown in the same medium supplemented with 1µg/ml of puromycin.

The RPMI 1640 and DMEM/F12 media contain 0.101 mM L-methionine and 0.208 mM L-cystine or 0.116 mM methionine and 0.1 mM L-cystine + 0.1 mM L-cysteine, respectively.

Cell viability assay

The cells were seeded in triplicate in 96-well plates at a density of 2×10^3 cells/well in 100 µL medium. Various concentrations of SeMet or SeCyt were added and plates were incubated at 37 °C for 24, 48, 72 or 96 h. Cell viability was assessed using the CellTiter 96® AQueous One Solution Cell Proliferation kit (Promega) as specified by the manufacturer on a Multiscan Spectrum spectrophotometer (Thermo LifeSciences), with absorbance read at 490 nm.

The L-methionine and L-cystine concentration in the media was varied by using a modified RPMI 1640 without glutamine, methionine and cystine (Sigma) supplemented with 2 mM L-glutamine, and either 0.1 mM methionine and varying concentrations of cystine, or 0.2 mM cystine and varying concentrations of methionine.

Apoptosis assay

The Annexin V-FITC (Fluorescein isothiocyanate)/Propidium Iodide (PI) staining/detection kit (Abcam) was used to measure apoptosis. MCF-10A cells were seeded in 6-well plates at a density of 5×10^5 cells/well and incubated at 37 °C with the specified concentrations of SeMet or SeCyt for 48 or 72 h. Cells were collected by trypsinization and culture supernatants were combined with trypsinized cells. After washing with PBS 1× , cells were resuspended in 200 µL annexin-binding buffer (10 mM Hepes pH 7.4, 140 mM NaCl, 2.5 mM $CaCl_2$) at a density of 5×10^5 cells/ml and stained with 2 µL each of Annexin V-FITC and PI for 15 min in dark tubes at room temperature. Flow cytometry analyses were performed immediately using a Guava easyCyte system (Millipore).

Western blot assay

MCF-10A cells were treated for 48 h with various concentrations of SeMet or SeCyt, collected by trypsinization and washed twice with PBS 1× . Cells were lysed at 4 °C for 15 min in RIPA buffer (50 mM Tris-HCl pH 7.5, 100 mM NaCl, 0.5% deoxycholate, 0.1% SDS, 1 % NP40)

containing 1 mM phenylmethylsulfonyl fluoride (PMSF) and protease inhibitors (0.5 µg/ml aprotinin, 0.5 µg/ml antipain, 0.5 µg/ml chymostatin, 0.5 µg/ml leupeptin, 0.5 µg/ml pepstatin A, 100 µg/ml benzamidine, 1 µg/ml *o*-phenantroline and 6 µg/ml ovomucoid). After centrifugation at 10000 g for 10 min, the supernatant was recovered and protein concentration in the cytoplasmic extracts was determined by the Bradford assay, using the Bio-Rad Protein Assay kit. 15 to 20 µg of proteins were loaded on 10 or 12 % polyacrylamide gels. Proteins were electrophoretically transferred onto nitrocellulose membranes (Whatman, BA85, 0.45 µm). After blocking in TBS buffer (10 mM Tris-HCl pH 8.0, 150 mM NaCl) containing 5% (w/v) skimmed milk, the nitrocellulose membranes were incubated overnight at 4 °C with primary antibodies in the same buffer, washed in TBS buffer containing 0.1% triton X-100, followed by incubation with secondary antibodies (horseradish peroxidase-conjugated anti-mouse or anti-rabbit antibodies) for 1 h at room temperature in TBS buffer containing 0.1% triton X-100. Signals were detected using the Lumi-Light Plus western Blotting Substrate (Roche) and quantified using Fiji.

Determination of free thiol content

MCF-10A cells were seeded in 6-well plates at a density of 1×10^6 cells/well and incubated at 37 °C with the specified concentrations of SeMet or SeCyt for 24h, collected by trypsinization and washed twice with PBS 1× . Cells were lysed at 4 °C for 15 min in 100 µL RIPA buffer, followed by centrifugation at 10000 g for 10 min. The supernatant was recovered and protein concentration in the cytoplasmic extracts was determined by the Bradford assay. 10% trichloracetic acid was added and the cell lysate was centrifuged at 10000 g for 10 min to precipitate the proteins. The supernatant was recovered and 20 µL was added to 580 µL solution containing 0.4 mM 5,5'-dithiobis-(2-nitrobenzoic acid) (DTNB) in 100 mM Tris-HCl pH 7.5.

Absorbance at 412 nm was recorded and thiol concentration (nmol/µg protein in the lysate) was determined by using a molar absorbance coefficient of 14,150 for 2-nitro-5-thiobenzoate.

Determination of the ER redox state

For preparation of stable cells expressing ER-targeted roGFP-S4, MCF-10A cells were transfected with pIRES-puro3-ERroGFP-S4 using JetPrime transfection reagent (Polyplus) and selected with 1µg/ml of puromycin. For imaging, MCF-10A cells stably expressing roGFP-S4 were seeded in 35 mm fibronectin-coated ibidi µ-dishes at 25 × 10^3 cells/dish and grown in medium without Phenol Red and puromycin with the indicated amount of selenoamino acids for 48 h or with 1 mM DTT or 1 mM Diamide for 15 min. Fluorescence images were acquired at 37°C using a confocal laser scanning microscope (TCS SP8, Leica) equipped with a high NA oil immersion objective (HC PL APO 63×/ 1.40, Leica), and a white light laser (WLL, Leica). The cells were excited using 405 nm and 442 nm lasers and their fluorescence was detected using a 500-587 nm filter. Confocal images were analyzed using a custom macro in the Fiji software. To analyze ER intensity in both channels, a mask of the ER was created using Triangle thresholding of the 405 nm excitation image. After background removal, the intensities were determined. The fluorescence ratios from excitation at 405 versus 442 nm were calculated in Fiji.

Statistical analysis

Results as presented as the mean values ± S. D. For t-tests, populations were first tested for Gaussian distribution using a Shapiro-Wilk Test with a α-value of 0.05. Because the compared populations were not all Gaussian, the difference between means was tested using a Mann–Whitney U test.

RESULTS

Selenoamino acid-mediated cytotoxicity

We evaluated L-SeMet and D,L-SeCyt toxicity in two cancer (Hela, MCF-7) and one non-cancerous breast epithelial (MCF-10A) cell lines, using an MTS (3-(4,5-dimethylthiazol-2-yl)-5-(3-carboxymethoxyphenyl)-2-(4-sulfophenyl)-2H-tetrazolium) cell proliferation assay. Growth in the presence of varying concentrations of selenoamino acids was assayed at different time points and the viability of treated versus untreated cells is reported in Fig. 1A. From these data, we obtained the IC_{50} values at 48, 72 and 96 h of exposure to SeMet and SeCyt (Table 1). Addition of low concentrations of SeMet or SeCyt slightly stimulated the growth of MCF-7 and MCF-10A cells, suggesting that the culture mediums are deficient in Se. At higher concentrations, both SeMet and SeCyt inhibited the proliferation of cells in a dose and time-dependent manner. The Hela cell line was the most sensitive to SeMet with an IC_{50} value at 72 h of 75 µM, compared to 140 µM and 200 µM, respectively for MCF-10A and MCF-7 cells. The data in Table 1 show that non-cancerous MCF-10A breast cells were more sensitive to SeMet than MCF-7 cancer cells. SeCyt was more toxic than SeMet in all the cell lines, with IC_{50} at 72 h in the 5 to 15 µM range compared to 100-200 µM for SeMet. MCF-10A cells were the most sensitive to SeCyt, with an IC_{50} value at 72 h of 4.5 µM. The MCF-7 cell line was the least sensitive to SeCyt with an IC_{50} value at 72 h of 15 µM.

Altogether, these results indicate that both selenoamino acids are as toxic in the normal MCF-10A cell line as in cancer Hela and MCF-7 cells, in contradiction with the assumption that Se compounds are selective for cancer cells [34].

Table 1 : IC_{50} values (µM) obtained from the viability data following exposure of Hela, MCF-7 or MCF-10A cells to L-Selenomethionine or D,L-Selenocystine in for 48, 72 or 96 h

	Se Compound					
	L-Selenomethionine (µM)			D,L-Selenocystine (µM)		
Cell line	IC_{50} 48 h	IC_{50} 72 h	IC_{50} 96 h	IC_{50} 48 h	IC_{50} 72 h	IC_{50} 96 h
Hela	120 ± 30	75 ± 8	60 ± 8	12 ± 3	6 ± 2	4 ± 1
MCF-7	>500	200 ± 25	120 ± 20	22 ± 4	15 ± 3	9 ± 2
MCF-10A	>500	140 ± 20	80 ± 12	8.5 ± 1	4.5 ± 0.5	3.5 ± 0.5

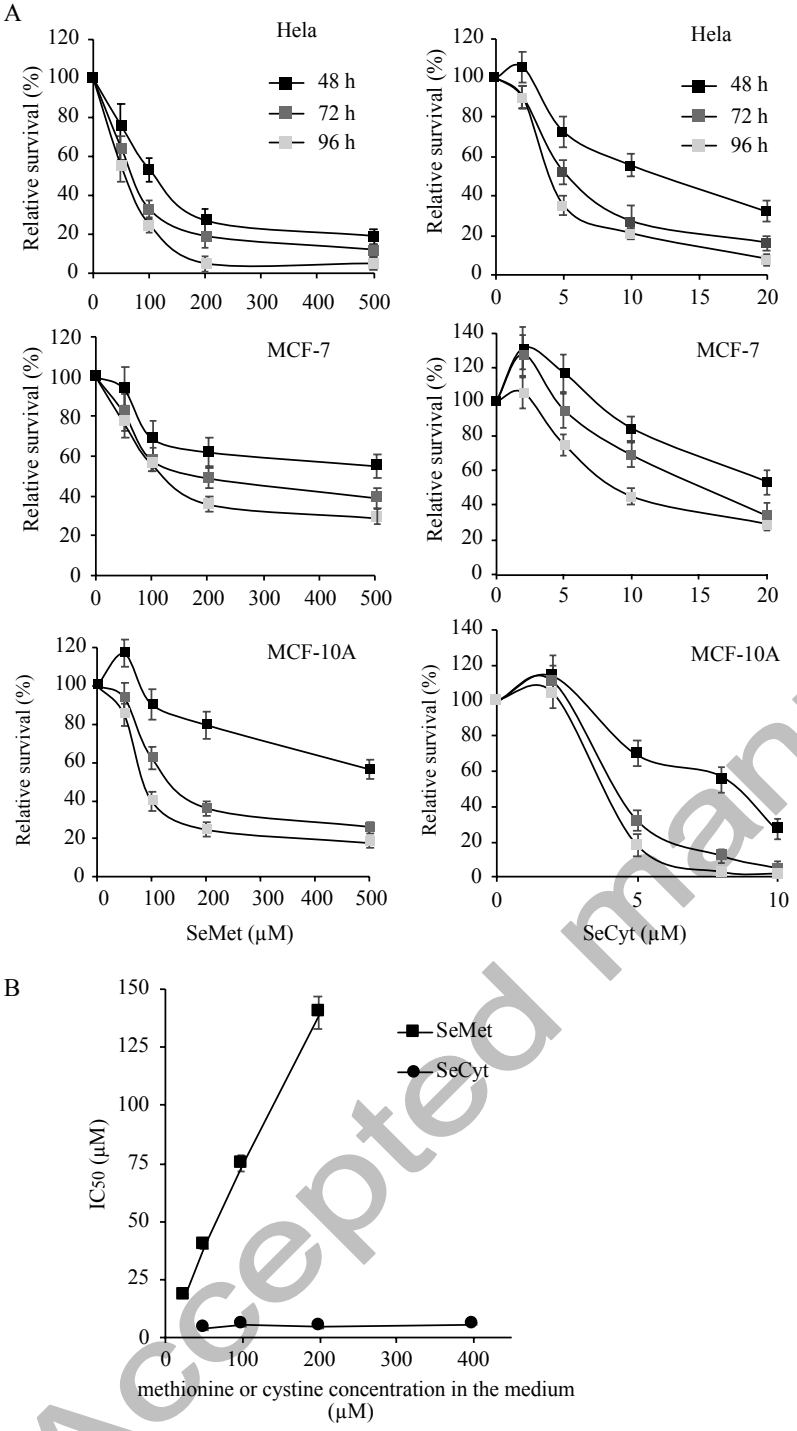

Figure 1. Cytotoxic effects of L-selenomethionine (SeMet) (left pannel) and D,L-selenocystine (SeCyt) (right pannel) on the growth of Hela, MCF-7 and MCF-10A cells

(A) Cell viability was measured using MTS (3-(4,5-dimethylthiazol-2-yl)-5-(3-carboxymethoxyphenyl)-2-(4-sulfophenyl)-2H-tetrazolium) following treatment with the indicated concentrations of SeMet or SeCyt for 48 (□), 72 (□) or 96 h (□). Relative values are expressed as percentage of viability of untreated cells. Viability was assessed in triplicate wells. Standard deviations, indicated by error bars, were determined from at least three independent experiments. (B) IC_{50} for SeMet (□) and SeCyt (☆) were obtained from the viability data from Hela cells grown 72 h in RPMI medium without methionine or cysteine and supplemented with increasing amounts of

the corresponding amino acid. Viability was assessed in triplicate wells. Standard deviations, indicated by error bars, were determined from three independent experiments.

It was previously demonstrated that SeMet toxicity depended on the methionine concentration in the growth medium, suggesting a competition between SeMet and methionine for uptake and along the downstream metabolic pathways inside the cell [30, 31]. Toxicity of SeCyt might similarly be affected by cystine levels in the medium. To evaluate the effect of varying the concentration of sulfur amino acids on the toxicity of SeMet and SeCyt, HeLa cells were grown in RPMI medium without methionine or cysteine and supplemented with increasing amounts of the corresponding amino acids (Fig. 1B). The toxicity of SeMet strictly depended on the SeMet/Met ratio, with IC_{50} at 72 h varying from 18 to 140 µM SeMet when the methionine concentration increased from 25 to 200 µM. The concentration of cystine in the medium (50 to 400 µM) had no effect on SeMet toxicity (result not shown). In contrast, the IC_{50} at 72 h for SeCyt remained at around 4-6 µM for cystine concentrations ranging from 50 to 400 µM. These results indicate that SeCyt is toxic *per se* and not because it enters in competition with cysteine for metabolic pathways such as protein synthesis.

Induction of apoptosis by SeMet and SeCyt in MCF-10A cells

Both SeMet and SeCyt were shown to induce apoptosis in several cancer cell lines [24, 35]. However, little is known on the cytotoxicity mechanisms of these Se compounds in a normal cell model. To investigate whether they induce apoptosis in MCF-10A, we used an annexin V/Propidium Iodide binding assay and quantified viable (Annexin V^-/ PI^-), early apoptotic (Annexin V^+/ PI^-) and late apoptotic/necrotic (Annexin V^+/PI^+) cells by flow cytometry (Fig 2A). As shown in Fig. 2B, upon exposure to SeMet or SeCyt for 48 or 72 hours, the proportion of early apoptotic cells increased in a dose and time-dependent manner. In the presence of 100 to 400 µM SeMet, the amount of late apoptotic/necrotic cells remained fairly constant, at around

20 % during the experiment, whereas these cells became more abundant as SeCyt concentration and time increased.

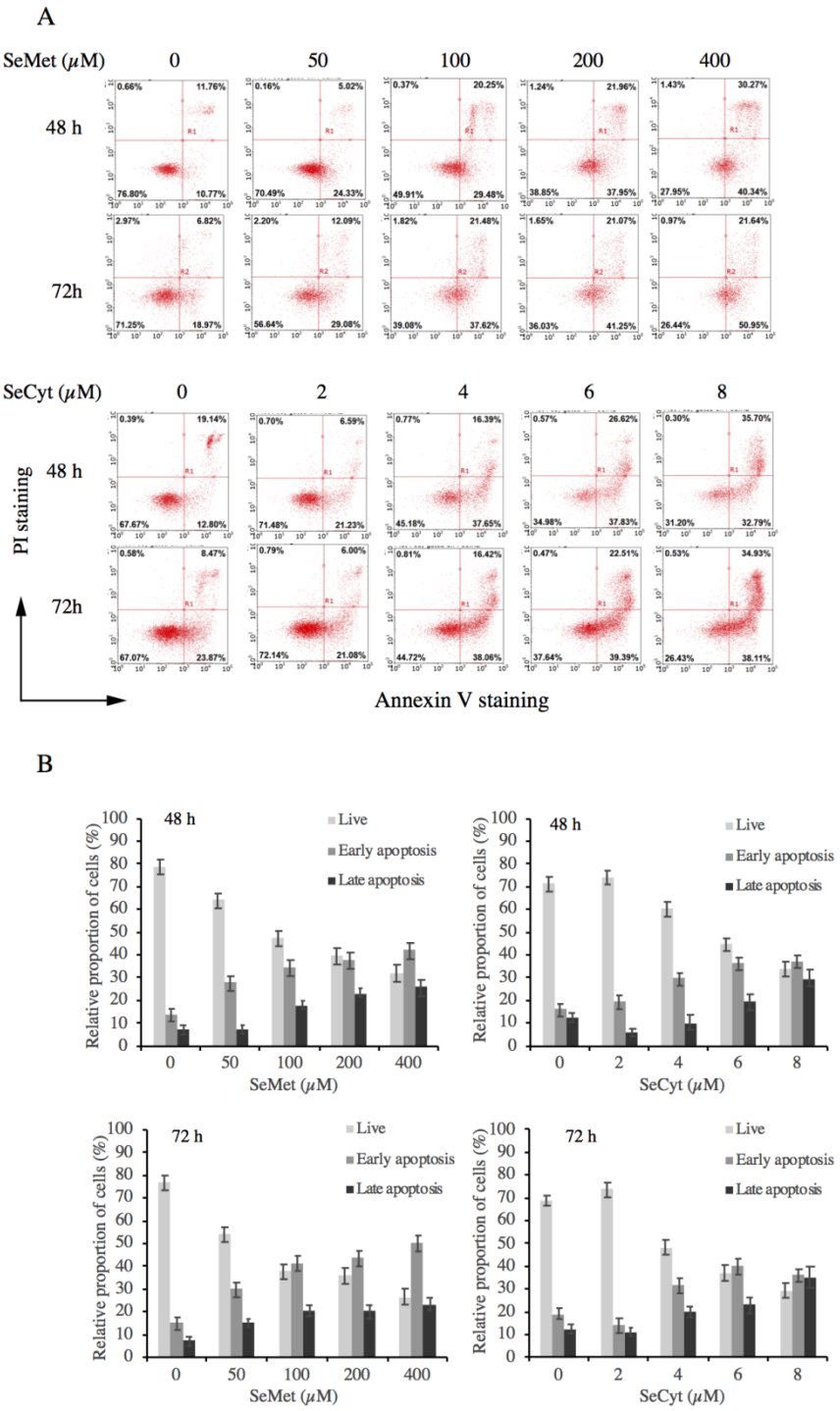

Figure 2. Evaluation of apoptosis in MCF-10A cells using Annexin V-PI double staining.

(A) Representative flow cytometry dot plots of apoptosis following treatment of MCF-10A cells with 0, 50, 100, 200 or 400 μM L-selenomethionine (SeMet) (upper panels) or 0, 2, 4, 6, or 8 μM D,L-selenocystine (SeCyt) (lower panels) for 48 and 72 h. Viable cells are seen in the left lower quadrant (FITC-/PI-), early apoptotic cells in the right lower quadrant (FITC+/PI-), and late apoptotic cells in the right upper quadrant (FITC+/PI+). The

percentage of cells in each quadrant is indicated. (B) Quantification of live (□), early apoptotic (▨) and late apoptotic (■) cells. Results are shown as mean ± SD from three experiments.

Cell signaling pathways involved in selenoamino acid-mediated cytotoxicity

To get more insights into the mechanisms of toxicity of selenoamino acids, we examined the importance of different stress response pathways for human cell survival. To that end, we analyzed the expression of specific targets of transcription factors controlling stress responses, in MCF-10A cells exposed for 48h to SeMet (0 to 300 µM) (Fig 3A) or SeCyt (0 to 5 µM) (Fig 3B). This range of concentration was chosen to ensure high viability with less than 20-25 % late apoptotic/ necrotic cells even at the highest concentration of Se.

NRF2 (nuclear factor erythroid related factor 2) is one of the major regulators of cellular defense against oxidative stress [36]. The activation of this pathway induces the transcription of a wide array of genes, including genes responsible for glutathione and thioredoxin production and regeneration. As shown in Fig. 3C, exposure to SeCyt up-regulated the expression of NRF2 in a dose-dependent manner. At 5 µM SeCyt, a concentration that resulted in 80% survival, as judged by the MTS assay, with around 30% of pre-apoptotic cells after 48h, the expression of NRF2 was induced *circa* 6 times. In contrast, SeMet up to 300 µM was unable to activate NRF2.

To determine whether cytosolic protein homeostasis was affected, we analyzed the expression of HSP27 (Heat shock protein 27), a small chaperone protein that is overexpressed in a variety of stress states that cause protein denaturation [37]. One of its functions is to stabilize protein conformation and promote the refolding of misfolded proteins. Whereas SeCyt had no effects on the level of HSP27, SeMet exposure slightly up-regulated the expression of this protein, although not in a dose-dependent manner (Fig 3D). Because HSP27 has been shown to perform many different functions in normal as well as stress conditions, the response to SeMet might be explained by a non-toxic effect of this compound.

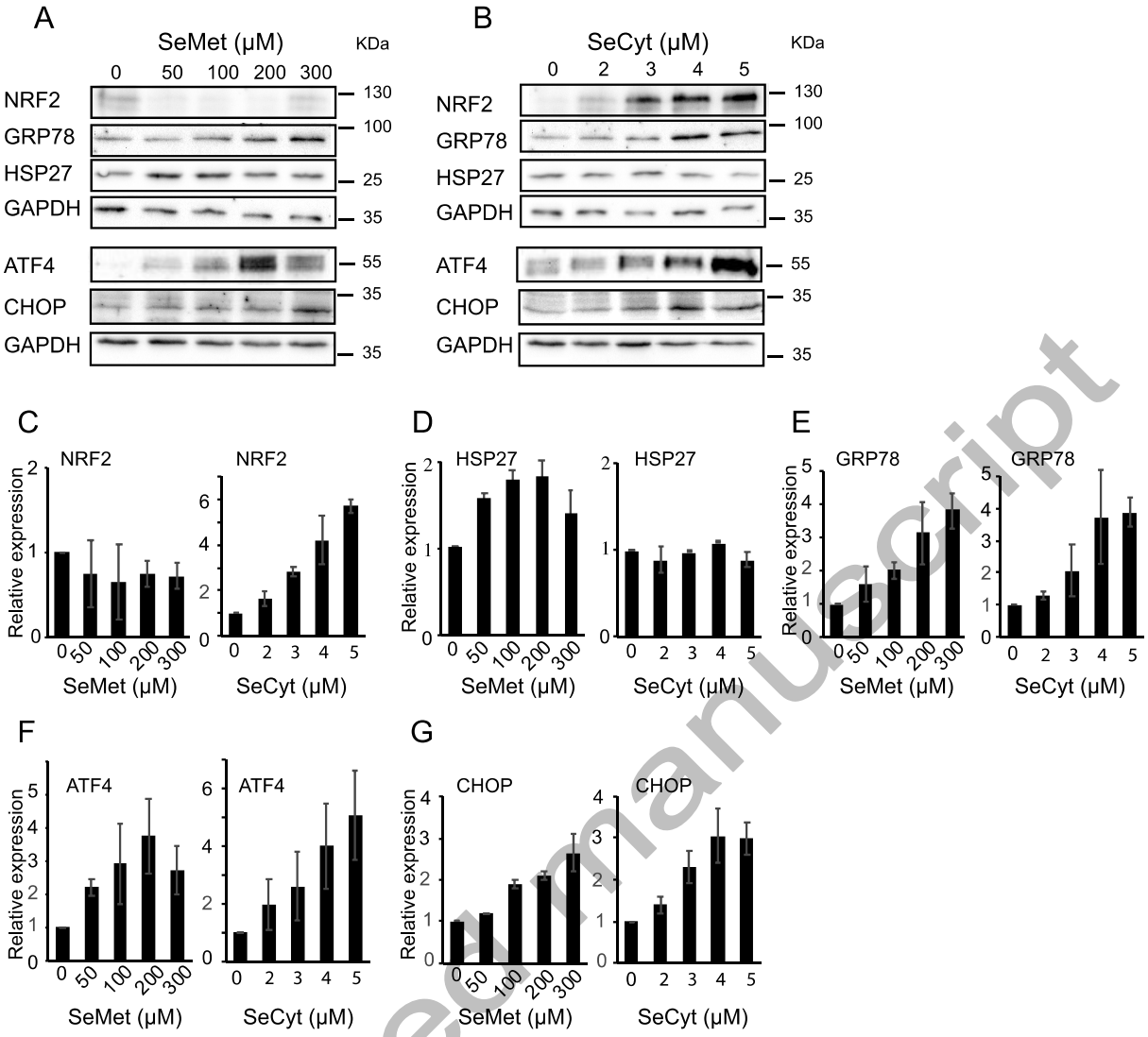

Figure 3. Western blot analysis of stress-related proteins in MCF-10A cells exposed to L-selenomethionine (SeMet) and D,L-selenocystine (SeCyt)

The expression of NRF2, GRP78, HSP27, ATF4 and CHOP was analyzed by Western blotting in MCF-10A cells exposed to 0 to 300 μM SeMet (A) and 0 to 5 μM SeCyt (B) for 48 h. GAPDH was used as a loading control. One representative image is shown. Densitometry analysis of NRF2 (C), HSP27 (D), GRP78 (E), ATF4 (F) and CHOP (G) were performed using the Fiji software on two western blot replicates from three independent experiments. Results were normalized to GAPDH (Glyceraldehyde 3-phosphate deshydrogenase). Error bars represent the mean and range of the results.

Because ER stress activation by the unfolded protein response (UPR) was shown to be involved in the anti-cancer properties of several Se compounds, we next examined the effect of SeMet and SeCyt on the expression of 78-kDa glucose-regulated protein (GRP78 also known as BiP). GRP78 is a UPR-upregulated ER chaperone that binds to secretory and transmembrane

precursor proteins to prevent their misfolding. In addition to its chaperoning function, GRP78 is also involved in regulating the UPR through its interaction with ER stress transducers IRE1 (inositol-requiring enzyme 1), ATF6 (activating transcription factor 6) and PERK (protein kinase R-like ER kinase). As shown in Fig. 3E, both SeMet and SeCyt up-regulated the expression of GRP78 in a dose-dependent manner, suggesting that both selenoamino acids act by disturbing ER protein homeostasis. To determine whether exposure to SeMet and SeCyt induced apoptosis via the UPR, we investigated the regulation of the ER stress-inducible transcription factor ATF4 and one of its target genes, the pro-apoptotic factor CCAAT/enhancer-binding protein homologous protein (CHOP). Both SeMet and SeCyt up-regulated the expression of ATF4 (Fig 3F) and CHOP (Fig 3G), suggesting that selenoamino acid-induced apoptosis may be triggered by ER stress.

Thiol oxidation mediated by selenoamino acid

Redox-active Se compounds can perform redox cycles involving low molecular weight thiols, resulting in massive oxidation of the cytosol and alteration of the intracellular redox balance [38]. SeCyt might induce an NRF2-mediated oxidative stress response by depleting intracellular thiols, as disruption of thiol homeostasis was shown to activate NRF2 [39]. To investigated this possibility, we quantified the concentration of free low molecular weight thiols in cells exposed to SeMet or SeCyt for 24 hours. We used highly toxic concentrations of selenoamino acids (up to 20 μM SeCyt and 1 mM SeMet) to maximize their potential effects. The amount of free thiols was measured in the supernatant of trichloracetic acid (TCA) precipitated cell extracts by reaction with DTNB. The results show that SeCyt, even at the lowest concentration used, induced a large depletion (> 50%) of low molecular weight thiols (Fig. 4A), whereas the amount of reduced thiols decreased only slightly (< 20%) in the presence

of SeMet (Fig. 4B). These results may explain why exposure to SeCyt triggers an oxidative stress response whereas exposure to SeMet does not.

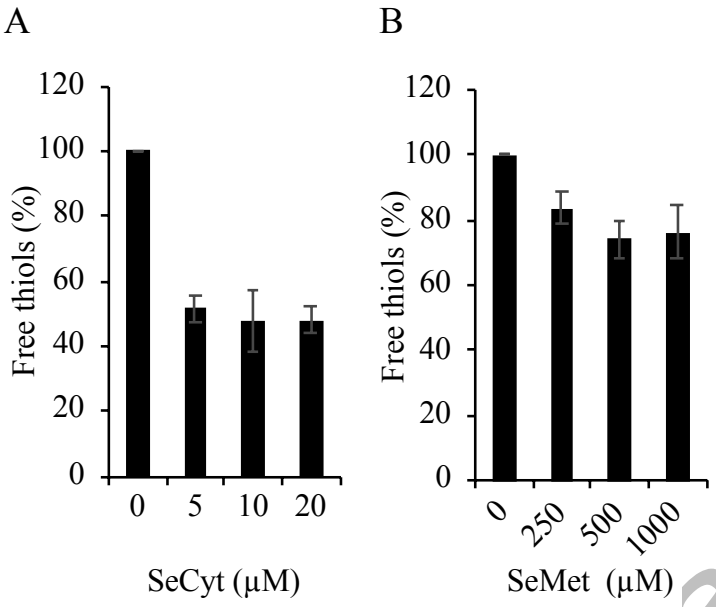

Figure 4. Low molecular weight (LMW) thiol content of MCF-10A cells

Cells were exposed to 0 to 20 µM D,L-selenocystine (SeCyt) (A) and 0 to 1 mM L-selenomethionine (SeMet) (B) for 24 h. The amount of LMW reduced thiols was measured by a DTNB assay in the supernatant of TCA precipitated cell extracts and expressed as percentage of thiols in untreated cells. A value of 0.100 ± 0.12 nmol thiol/µg protein was measured in untreated cells. The error bar represent the mean and range of three experiments.

The ER redox state is disturbed by SeMet and SeCyt

Oxidative protein folding requires an appropriate redox environment in the ER. We speculated that redox metabolites generated from SeMet and SeCyt may induce ER stress by altering the redox balance in the ER.

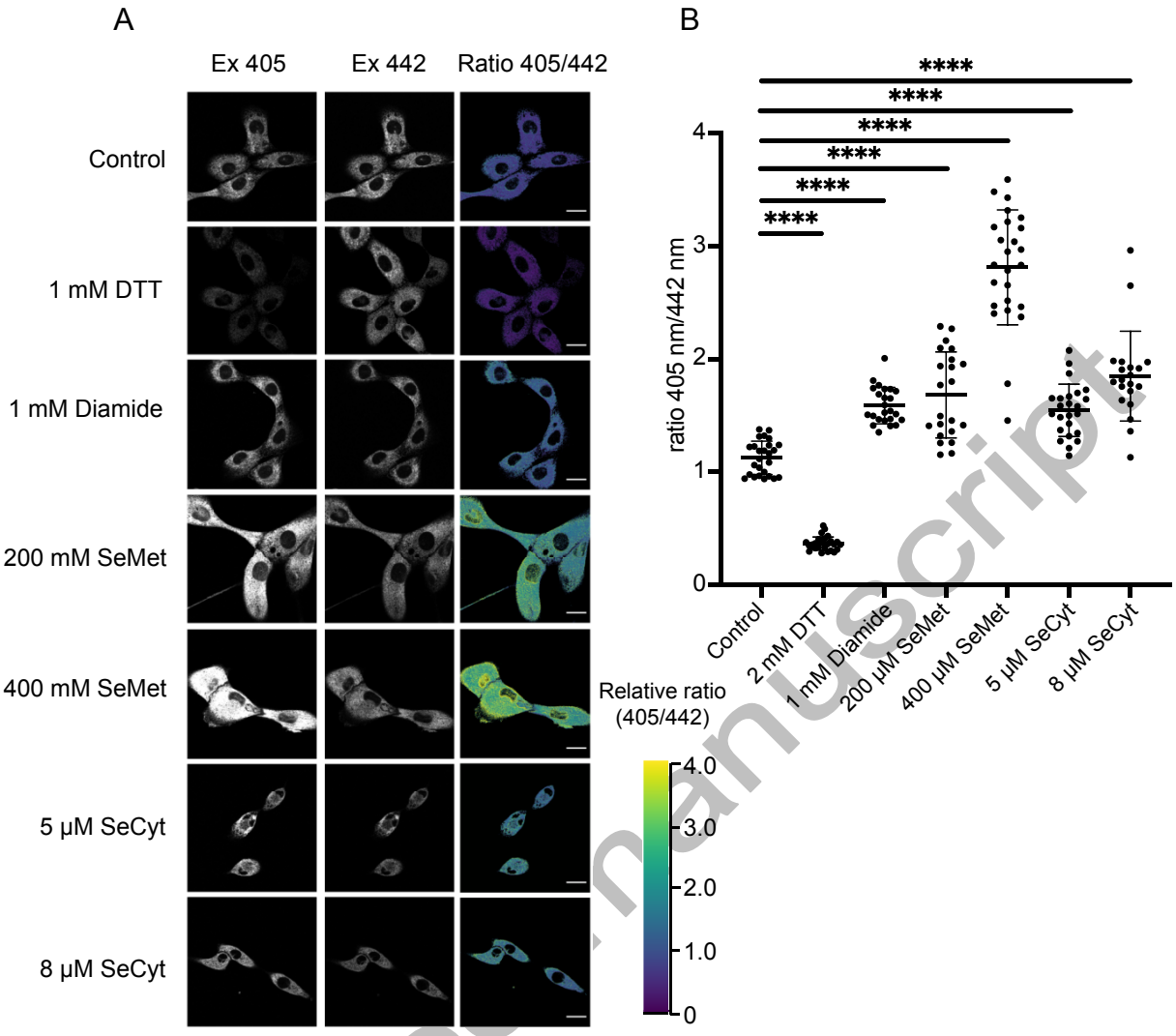

Figure 5. Fluorescence imaging of MCF-10A cells stably expressing ERroGFP-S4

(A) Representative fluorescence images of cells excited at 405 nm and 442 nm following treatments with nothing (control), 1 mM DTT or 1 mM Diamide for 15 min, or L-selenomethionine (SeMet) (200 and 400 µM) or D,L-selenocystine (SeCyt) (5 and 8 µM) for 48 h. The relative ratios of fluorescence intensities (Ratio 405/442) were calculated in Fiji and are shown with an arbitrary color scale. Scale bar is 10 µM. (B) Quantification of the intensity ratios were performed on at least 20 cells for each conditions. The results presented in the figure are from one experiment out of three which gave similar results. **** $p<0.0001$

To monitor the ER redox state in live cells, we established a stable MCF-10A cell line expressing the fluorescence redox probe ERroGFP-S4 constructed by Hoseki et al, which indicates ER redox state in real time [33]. Fluorescence images in the stable cell lines excited at 405 nm and 442 nm were observed under confocal microscopy, following treatments with

SeMet and SeCyt for 48 h or 1 mM DTT and 1 mM Diamide for 15 min as controls. As shown in Fig. 5A, cells displayed an ER-localized fluorescence that was responsive to changes in both reduction and oxidation. The fluorescence intensity ratio (Ratio 405/442) was quantified in at least 20 cells per condition (Fig 5B). An average ratio value of 1.1 ± 0.15 was determined in untreated cells. This value decreased to 0.4 ± 0.06 when cells were treated with DTT and increased to 1.6 ± 0.15 in the presence of diamide. Treatment with 5 μM or 8 μM SeCyt increased the average fluorescence ratio to 1.5 ± 0.2 and 1.8 ± 0.4, respectively. Surprisingly, the fluorescence ratio increased to 1.7 ± 0.4 and 2.8 ± 0.5 after 48 h in the presence of 200 μM and 400 μM SeMet, respectively, indicating that exposure to SeMet resulted in a strongly oxidized ER. These results show that both selenoamino acids disturb the ER redox state.

DISCUSSION

The purpose of this study was to get more insights into the molecular mechanisms underlying the response to selenoamino acid exposure in normal human cells and, in particular, to explore the hypothesis that, as reported previously in yeast, disruption of protein homeostasis due to SeCys misincorporation in proteins contributes to SeMet toxicity.

A great variability of results were reported on the SeMet dose necessary to elicit toxicity in cultured cells, with IC_{50} values ranging from a few µM to tenths of mM, depending on the cell type, culture conditions and type of assay [24]. In this study, we show that the IC_{50} value for SeMet varies as a function of the concentration of methionine in the culture medium and the time of exposure, which may partly explain the observed disparity between different studies. Therefore, it is important to take into account the SeMet/Met ratio rather than the selenium concentration only, when comparing the toxic effects of SeMet in various conditions. We show that both SeMet and SeCyt inhibit the growth of non-cancerous breast epithelial MCF-10A cells in the same concentration range as cancerous breast epithelial MCF-7 and Hela cells, in contradiction with the widespread belief that Se-containing compounds exhibit high selectivity towards cancer over normal cells [18, 35]. It was, indeed, reported that SeMet and SeCyt display little toxicity in normal fibroblast cells [40, 41]. The high cytotoxicity of selenoamino acids observed in this study may be cell type-specific. Previous reports indicate that several Se-containing compounds show low selectivity when comparing normal breast MCF-10A cells *vs* cancer breast MCF-7 cells [42, 43]. These results might be explained by the high proliferation rate (doubling time < 20 h in our conditions) of MCF-10A cells. A strong demand for amino acids and an enhanced metabolism to sustain high level of protein synthesis and DNA replication may underlie the cytotoxicity of selenoamino acids in fast growing cells in culture [44].

When cells are stressed, they initiate a complex and precisely tuned response to prevent permanent damage. Cellular proteostasis is maintained by stress-responsive signaling pathways such as the heat shock response (HSR), the oxidative stress response (OSR), and the unfolded protein response (UPR), which is activated upon accumulation of misfolded proteins in the ER [45]. Activation of these pathways results in the transcriptional upregulation of select subsets of stress-responsive genes that aim to promote recovery following various types of acute insult. We have previously shown that SeMet exposure in *S. cerevisiae* caused a proteotoxic stress and induced the expression of protein chaperones under the control of the heat-shock factor Hsf1p [32]. In MCF-10A cells, neither SeMet nor SeCyt toxicity was dependent on the concentration of cystine in the growth medium. This implies that competition between SeCys and cysteine for utilization in translation does not contribute significantly to SeCys (or SeMet) cytotoxicity. Moreover, exposure to SeCyt did not up-regulate the expression of HSP27, a chaperone involved in the refolding of misfolded protein, that is transcriptionally regulated by the heat shock transcription factor [46]. These results suggest that cytosolic accumulation of protein aggregates, caused by SeCys misincorporation in the place of cysteine, is not a major determinant of selenoamino acid cytotoxicity in human cells. Instead, exposure to SeCyt elicited a large depletion of intracellular free thiols as previously reported in HepG2 hepatoma cells [38], associated with the up-regulation of the expression of the oxidative stress pathway transcription factor NRF2. This result confirms a previous report showing nuclear translocation of NRF2 and induction of NRF2 target genes in human BEAS-2B lung cells exposed to SeCyt [47]. These effects are most likely due to the efficient GSH reduction of SeCyt to SeCys and subsequent redox cycling of the selenol/diselenide couple with oxygen and thiols, producing ROS and promoting redox imbalance [48]. These results are in agreement with the generally accepted hypothesis that the cytotoxic effects of selenium compounds derive from their ability or that of their metabolites to produce an accumulation of ROS. Previous reports have, indeed,

demonstrated SeCyt induction of apoptosis through ROS-mediated DNA damage in various human cells [41, 49-51].

In addition, we show that both SeMet and SeCyt up-regulated the expression of the UPR major target GRP78, ER stress-regulated transcription factor ATF4 and its downstream target CHOP, a transcription factor implicated in the control of translation and apoptosis [52], suggesting that ER stress also plays a role in selenoamino acid-induced apoptosis. Several reports have documented the role of ER stress in mediating the apoptotic effect of Se-containing compounds [26, 53-57]. In particular, SeCyt exposure was shown to alter the expression of ER stress-regulated proteins in Hela cells [58]. Disulfide-bond formation is required for structural formation and functions of many proteins that are folded and maturated in the ER. This process is achieved through a series of thiol-disulfide exchange reactions between substrate polypeptides and the oxidized form of protein disulfide isomerase (PDI), which in turn is oxidized by the ER oxidase Ero1L [59]. Compared with the cytosol, the ER keeps an oxidative environment suitable for oxidative protein folding. This process is exquisitely sensitive to redox perturbations of the ER lumen environment as both hyperoxidizing and reductive challenges were shown to activate ER stress signaling [60]. In this study, using a redox-sensitive fluorescent probe targeted to the ER [33], we show that both selenoamino acids shifted the ER redox balance towards an even more oxidizing environment. Redox cycling of SeCys with GSH in the ER should result in a lower GSH/GSSG ratio leading to an oxidative shift, impaired disulfide bond formation and activation of the UPR. On the other hand, how SeMet, which is not redox active, can oxidize the ER remains to be established. Several reports indicate that SeMet effects could be mediated by ROS originating from its metabolization to methylselenol (MeSeH), by methionine- ■-lyase activity [61, 62]. However, speciation studies in rat liver or in human leukemia cells exposed to SeMet failed to detect MeSeH suggesting that metabolization of SeMet to MeSeH is insignificant in animals [63, 64]. Moreover, in a previous

report, we showed that, in *S. cerevisiae,* exposure to MeSeH triggered a reductive shift in the ER rather than oxidation [65]. These observations do not support a role for MeSeH as a toxic metabolic intermediate of SeMet. Another possibility is that SeMet effects are mediated by selenohomocysteine, which is a natural metabolite of SeMet produced by the methionine cycle and, like selenocysteine, is capable of redox cycling with GSH. Additional studies, such as exploring the signaling pathways activated by direct exposure to selenohomocystine, are necessary to answer this question.

LEGEND TO THE FIGURES

Figure 1. Cytotoxic effects of L-selenomethionine (SeMet) (left pannel) and D,L-selenocystine (SeCyt) (right pannel) on the growth of Hela, MCF-7 and MCF-10A cells

(A) Cell viability was measured using MTS (3-(4,5-dimethylthiazol-2-yl)-5-(3-carboxymethoxyphenyl)-2-(4-sulfophenyl)-2H-tetrazolium) following treatment with the indicated concentrations of SeMet or SeCyt for 48 (□), 72 (□) or 96 h (□). Relative values are expressed as percentage of viability of untreated cells. Viability was assessed in triplicate wells. Standard deviations, indicated by error bars, were determined from at least three independent experiments. (B) IC_{50} for SeMet (□) and SeCyt (★) were obtained from the viability data from Hela cells grown 72 h in RPMI medium without methionine or cysteine and supplemented with increasing amounts of the corresponding amino acid. Viability was assessed in triplicate wells. Standard deviations, indicated by error bars, were determined from three independent experiments.

Figure 2. Evaluation of apoptosis in MCF-10A cells using Annexin V-PI double staining.

(A) Representative flow cytometry dot plots of apoptosis following treatment of MCF-10A cells with 0, 50, 100, 200 or 400 µM **L-selenomethionine (**SeMet) (upper panels) or 0, 2, 4, 6, or 8 µM **D,L-selenocystine** (SeCyt) (lower panels) for 48 and 72 h. Viable cells are seen in the left lower quadrant (FITC-/PI-), early apoptotic cells in the right lower quadrant (FITC+/PI-), and late apoptotic cells in the right upper quadrant (FITC+/PI+). The percentage of cells in each quadrant is indicated. (B) Quantification of live (□), early apoptotic (□) and late apoptotic (□) cells. Results are shown as mean ± SD from three experiments.

Figure 3. Western blot analysis of stress-related proteins in MCF-10A cells exposed to L-selenomethionine (SeMet) and D,L-selenocystine (SeCyt) The expression of NRF2, GRP78, HSP27, ATF4 and CHOP was analyzed by Western blotting in MCF-10A cells exposed to 0 to 300 µM SeMet (A) and 0 to 5 µM SeCyt (B) for 48 h. GAPDH was used as a loading control. One representative image is shown. Densitometry analysis of NRF2 (C), HSP27 (D), GRP78 (E), ATF4 (F) and CHOP (G) were performed using the Fiji software on two western blot replicates from three independent experiments. Results were normalized to GAPDH (Glyceraldehyde 3-phosphate deshydrogenase). Error bars represent the mean and range of the results.

Figure 4. Low molecular weight thiol content of MCF-10A cells

Cells were exposed to 0 to 20 µM **D,L-selenocystine (SeCyt)** (A) and 0 to 1 mM **L-selenomethionine (SeMet)** (B) for 24 h. The amount of LMW reduced thiols was measured by a DTNB assay in the supernatant of TCA precipitated cell extracts and expressed as percentage of thiols in untreated cells. A value of 0.100 ± 0.12 nmol thiol/µg protein was measured in untreated cells. The error bar represent the mean and range of three experiments.

Figure 5. Fluorescence imaging of MCF-10A cells stably expressing ERroGFP-S4

(A) Representative fluorescence images of cells excited at 405 nm and 442 nm following treatments with nothing (control), 1 mM DTT or 1 mM Diamide for 15 min, or **L-selenomethionine (SeMet)** (200 and 400 µM) or **D,L-selenocystine (SeCyt)** (5 and 8 µM) for 48 h. The relative ratios of fluorescence intensities (Ratio 405/442) were calculated in Fiji and are shown with an arbitrary color scale. Scale bar is 10 µM. (B) Quantification of the intensity ratios were performed on at least 20 cells for each conditions. The results presented in the figure are from one experiment out of three which gave similar results. **** $p<0.0001$

REFERENCES

1. Hatfield DL, Tsuji PA, Carlson BA, Gladyshev VN. Selenium and selenocysteine: roles in cancer, health, and development. *Trends Biochem Sci*. 2014;39(3):112-120. doi:10.1016/j.tibs.2013.12.007
2. Labunskyy VM, Hatfield DL, Gladyshev VN. Selenoproteins: molecular pathways and physiological roles. *Physiol Rev*. 2014;94(3):739-777. doi:10.1152/physrev.00039.2013
3. Loscalzo J. Keshan disease, selenium deficiency, and the selenoproteome. *N Engl J Med*. 2014;370(18):1756-1760. doi:10.1056/NEJMcibr1402199
4. Shimada BK, Alfulaij N, Seale LA. The Impact of Selenium Deficiency on Cardiovascular Function. *Int J Mol Sci*. 2021;22(19)doi:10.3390/ijms221910713
5. Rayman MP. Selenium in cancer prevention: a review of the evidence and mechanism of action. *Proc Nutr Soc*. 2005;64(4):527-542.
6. Skalickova S, Milosavljevic V, Cihalova K, Horky P, Richtera L, Adam V. Selenium nanoparticles as a nutritional supplement. *Nutrition*. 2017;33:83-90. doi:https://doi.org/10.1016/j.nut.2016.05.001
7. Kieliszek M, Serrano Sandoval SN. The importance of selenium in food enrichment processes. A comprehensive review. *J Trace Elem Med Biol*. 2023;79:127260. doi:10.1016/j.jtemb.2023.127260
8. Vinceti M, Filippini T, Del Giovane C, et al. Selenium for preventing cancer. *Cochrane Database of Systematic Reviews*. 2018;(1)doi:10.1002/14651858.CD005195.pub4
9. Rayman MP, Winther KH, Pastor-Barriuso R, et al. Effect of long-term selenium supplementation on mortality: Results from a multiple-dose, randomised controlled trial. *Free Radic Biol Med*. 2018;127:46-54. doi:10.1016/j.freeradbiomed.2018.02.015
10. Vinceti M, Filippini T, Wise LA. Environmental Selenium and Human Health: an Update. *Curr Environ Health Rep*. 2018;5(4):464-485. doi:10.1007/s40572-018-0213-0
11. Rayman MP. Selenium intake, status, and health: a complex relationship. *Hormones (Athens)*. 2020;19(1):9-14. doi:10.1007/s42000-019-00125-5
12. Spallholz JE. Free radical generation by selenium compounds and their prooxidant toxicity. *Biomed Environ Sci*. 1997;10(2-3):260-270.
13. Seko Y, Imura N. Active oxygen generation as a possible mechanism of selenium toxicity. *Biomed Environ Sci*. 1997;10(2-3):333-339.
14. Drake EN. Cancer chemoprevention: selenium as a prooxidant, not an antioxidant. *Med Hypotheses*. 2006;67(2):318-322. doi:10.1016/j.mehy.2006.01.058
15. Tarze A, Dauplais M, Grigoras I, et al. Extracellular production of hydrogen selenide accounts for thiol-assisted toxicity of selenite against Saccharomyces cerevisiae. *J Biol Chem*. 2007;282(12):8759-8767. doi:10.1074/jbc.M610078200
16. Kumar S, Björnstedt M, Holmgren A. Selenite is a substrate for calf thymus thioredoxin reductase and thioredoxin and elicits a large non-stoichiometric oxidation of NADPH in the presence of oxygen. *Eur J Biochem*. 1992;207(2):435-439.
17. Misra S, Boylan M, Selvam A, Spallholz JE, Björnstedt M. Redox-active selenium compounds—from toxicity and cell death to cancer treatment. *Nutrients*. 2015;7(5):3536-3556. doi:10.3390/nu7053536
18. Fernandes AP, Gandin V. Selenium compounds as therapeutic agents in cancer. *Biochim Biophys Acta*. 2015;1850(8):1642-1660. doi:10.1016/j.bbagen.2014.10.008
19. Hondal RJ, Marino SM, Gladyshev VN. Selenocysteine in thiol/disulfide-like exchange reactions. *Antioxid Redox Signal*. 2013;18(13):1675-1689. doi:10.1089/ars.2012.5013
20. Kuršvietienė L, Mongirdienė A, Bernatonienė J, Šulinskienė J, Stanevičienė I. Selenium Anticancer Properties and Impact on Cellular Redox Status. *Antioxidants (Basel)*. 2020;9(1)doi:10.3390/antiox9010080

21. Stolwijk JM, Garje R, Sieren JC, Buettner GR, Zakharia Y. Understanding the Redox Biology of Selenium in the Search of Targeted Cancer Therapies. *Antioxidants*. 2020;9(5):420.
22. Dauplais M, Bierla K, Maizeray C, et al. Methylselenol Produced In Vivo from Methylseleninic Acid or Dimethyl Diselenide Induces Toxic Protein Aggregation in Saccharomyces cerevisiae. *Int J Mol Sci*. 2021;22(5):2241. doi:10.3390/ijms22052241
23. Schrauzer GN. The nutritional significance, metabolism and toxicology of selenomethionine. *Adv Food Nutr Res*. 2003;47:73-112.
24. Lazard M, Dauplais M, Blanquet S, Plateau P. Recent advances in the mechanism of selenoamino acids toxicity in eukaryotic cells. *Biomol Concepts*. 2017;8(2):93-104. doi:10.1515/bmc-2017-0007
25. Suzuki M, Endo M, Shinohara F, Echigo S, Rikiishi H. Rapamycin suppresses ROS-dependent apoptosis caused by selenomethionine in A549 lung carcinoma cells. *Cancer Chemother Pharmacol*. 2011;67(5):1129-1136. doi:10.1007/s00280-010-1417-7
26. Suzuki M, Endo M, Shinohara F, Echigo S, Rikiishi H. Differential apoptotic response of human cancer cells to organoselenium compounds. *Cancer Chemother Pharmacol*. 2010;66(3):475-484. doi:10.1007/s00280-009-1183-6
27. Korbut E, Ptak-Belowska A, Brzozowski T. Inhibitory effect of selenomethionine on carcinogenesis in the model of human colorectal cancer in vitro and its link to the Wnt/β-catenin pathway. *Acta Biochim Pol*. 2018;65(3):359-366. doi:10.18388/abp.2018_2628
28. Zhang B, Wei X, Li J. Selenomethionine suppresses head and neck squamous cell carcinoma progression through TopBP1/ATR and TCAB1 signaling. *Histol Histopathol*. 2023:18665. doi:10.14670/hh-18-665
29. Ouerdane L, Mester Z. Production and characterization of fully selenomethionine-labeled *Saccharomyces cerevisiae*. *J Agric Food Chem*. 2008;56(24):11792-11799. doi:10.1021/jf8018479
30. Kajander EO, Harvima RJ, Eloranta TO, et al. Metabolism, cellular actions, and cytotoxicity of selenomethionine in cultured cells. *Biol Trace Elem Res*. 1991;28(1):57-68.
31. Lazard M, Dauplais M, Blanquet S, Plateau P. Trans-sulfuration pathway seleno-amino acids are mediators of selenomethionine toxicity in *Saccharomyces cerevisiae*. *J Biol Chem*. 2015;290(17):10741-10750. doi:10.1074/jbc.M115.640375
32. Plateau P, Saveanu C, Lestini R, et al. Exposure to selenomethionine causes selenocysteine misincorporation and protein aggregation in Saccharomyces cerevisiae. *Sci Rep*. 2017;7:44761. doi:10.1038/srep44761
33. Hoseki J, Oishi A, Fujimura T, Sakai Y. Development of a stable ERroGFP variant suitable for monitoring redox dynamics in the ER. *Biosci Rep*. 2016;36(2)doi:10.1042/bsr20160027
34. Wallenberg M, Misra S, Björnstedt M. Selenium cytotoxicity in cancer. *Basic Clin Pharmacol Toxicol*. 2014;114(5):377-386. doi:10.1111/bcpt.12207
35. Gandin V, Khalkar P, Braude J, Fernandes AP. Organic selenium compounds as potential chemotherapeutic agents for improved cancer treatment. *Free Radical Biology and Medicine*. 2018;127:80-97. doi:https://doi.org/10.1016/j.freeradbiomed.2018.05.001
36. Suzuki T, Takahashi J, Yamamoto M. Molecular Basis of the KEAP1-NRF2 Signaling Pathway. *Mol Cells*. 2023;46(3):133-141. doi:10.14348/molcells.2023.0028
37. Zou Y, Shi H, Liu N, Wang H, Song X, Liu B. Mechanistic insights into heat shock protein 27, a potential therapeutic target for cardiovascular diseases. *Front Cardiovasc Med*. 2023;10:1195464. doi:10.3389/fcvm.2023.1195464
38. Kim TS, Yun BY, Kim IY. Induction of the mitochondrial permeability transition by selenium compounds mediated by oxidation of the protein thiol groups and generation of the superoxide. *Biochem Pharmacol*. 2003;66(12):2301-2311.

39. Cvetko F, Caldwell ST, Higgins M, et al. Nrf2 is activated by disruption of mitochondrial thiol homeostasis but not by enhanced mitochondrial superoxide production. *J Biol Chem*. 2021;296:100169. doi:10.1074/jbc.RA120.016551
40. Redman C, Scott JA, Baines AT, et al. Inhibitory effect of selenomethionine on the growth of three selected human tumor cell lines. *Cancer Lett*. 1998;125(1-2):103-110.
41. Chen T, Wong YS. Selenocystine induces reactive oxygen species-mediated apoptosis in human cancer cells. *Biomed Pharmacother*. 2009;63(2):105-113. doi:10.1016/j.biopha.2008.03.009
42. da Costa NS, Lima LS, Oliveira FAM, et al. Antiproliferative Effect of Inorganic and Organic Selenium Compounds in Breast Cell Lines. *Biomedicines*. 2023;11(5)doi:10.3390/biomedicines11051346
43. Ibáñez E, Plano D, Font M, et al. Synthesis and antiproliferative activity of novel symmetrical alkylthio- and alkylseleno-imidocarbamates. *Eur J Med Chem*. 2011;46(1):265-274. doi:10.1016/j.ejmech.2010.11.013
44. DeBerardinis RJ, Chandel NS. Fundamentals of cancer metabolism. *Sci Adv*. 2016;2(5):e1600200. doi:10.1126/sciadv.1600200
45. Fulda S, Gorman AM, Hori O, Samali A. Cellular stress responses: cell survival and cell death. *Int J Cell Biol*. 2010;2010:214074. doi:10.1155/2010/214074
46. de Thonel A, Le Mouël A, Mezger V. Transcriptional regulation of small HSP-HSF1 and beyond. *Int J Biochem Cell Biol*. 2012;44(10):1593-1612. doi:10.1016/j.biocel.2012.06.012
47. Poerschke RL, Franklin MR, Moos PJ. Modulation of redox status in human lung cell lines by organoselenocompounds: selenazolidines, selenomethionine, and methylseleninic acid. *Toxicol In Vitro*. 2008;22(7):1761-1767. doi:10.1016/j.tiv.2008.08.003
48. Rahmanto AS, Davies MJ. Selenium-containing amino acids as direct and indirect antioxidants. *IUBMB Life*. 2012;64(11):863-871. doi:10.1002/iub.1084
49. Chen T, Wong YS. Selenocystine induces S-phase arrest and apoptosis in human breast adenocarcinoma MCF-7 cells by modulating ERK and Akt phosphorylation. *J Agric Food Chem*. 2008;56(22):10574-10581. doi:10.1021/jf802125t
50. Chen T, Wong YS. Selenocystine induces caspase-independent apoptosis in MCF-7 human breast carcinoma cells with involvement of p53 phosphorylation and reactive oxygen species generation. *Int J Biochem Cell Biol*. 2009;41(3):666-676. doi:10.1016/j.biocel.2008.07.014
51. Wahyuni EA, Yii CY, Liang HL, et al. Selenocystine induces oxidative-mediated DNA damage via impairing homologous recombination repair of DNA double-strand breaks in human hepatoma cells. *Chem Biol Interact*. 2022;365:110046. doi:10.1016/j.cbi.2022.110046
52. Hu H, Tian M, Ding C, Yu S. The C/EBP Homologous Protein (CHOP) Transcription Factor Functions in Endoplasmic Reticulum Stress-Induced Apoptosis and Microbial Infection. *Front Immunol*. 2018;9:3083. doi:10.3389/fimmu.2018.03083
53. Wu Y, Zhang H, Dong Y, Park YM, Ip C. Endoplasmic reticulum stress signal mediators are targets of selenium action. *Cancer Res*. 2005;65(19):9073-9079. doi:10.1158/0008-5472.Can-05-2016
54. Zu K, Bihani T, Lin A, Park YM, Mori K, Ip C. Enhanced selenium effect on growth arrest by BiP/GRP78 knockdown in p53-null human prostate cancer cells. *Oncogene*. 2006;25(4):546-554. doi:10.1038/sj.onc.1209071
55. Shigemi Z, Manabe K, Hara N, et al. Methylseleninic acid and sodium selenite induce severe ER stress and subsequent apoptosis through UPR activation in PEL cells. *Chem Biol Interact*. 2017;266:28-37. doi:10.1016/j.cbi.2017.01.027

56. Goltyaev MV, Mal'tseva VN, Varlamova EG. Expression of ER-resident selenoproteins and activation of cancer cells apoptosis mechanisms under ER-stress conditions caused by methylseleninic acid. *Gene*. 2020;755:144884. doi:10.1016/j.gene.2020.144884
57. Zachariah M, Maamoun H, Milano L, Rayman MP, Meira LB, Agouni A. Endoplasmic reticulum stress and oxidative stress drive endothelial dysfunction induced by high selenium. *J Cell Physiol*. 2021;236(6):4348-4359. doi:10.1002/jcp.30175
58. Wallenberg M, Misra S, Wasik AM, et al. Selenium induces a multi-targeted cell death process in addition to ROS formation. *J Cell Mol Med*. 2014;18(4):671-684. doi:10.1111/jcmm.12214
59. Wang L, Wang CC. Oxidative protein folding fidelity and redoxtasis in the endoplasmic reticulum. *Trends Biochem Sci*. 2023;48(1):40-52. doi:10.1016/j.tibs.2022.06.011
60. Eletto D, Chevet E, Argon Y, Appenzeller-Herzog C. Redox controls UPR to control redox. *J Cell Sci*. 2014;127(Pt 17):3649-3658. doi:10.1242/jcs.153643
61. Okuno T, Kubota T, Kuroda T, Ueno H, Nakamuro K. Contribution of enzymic alpha, gamma-elimination reaction in detoxification pathway of selenomethionine in mouse liver. *Toxicol Appl Pharmacol*. 2001;176(1):18-23. doi:10.1006/taap.2001.9260
62. Palace VP, Spallholz JE, Holm J, Wautier K, Evans RE, Baron CL. Metabolism of selenomethionine by rainbow trout (Oncorhynchus mykiss) embryos can generate oxidative stress. *Ecotoxicol Environ Saf*. 2004;58(1):17-21. doi:10.1016/j.ecoenv.2003.08.019
63. Suzuki KT, Kurasaki K, Suzuki N. Selenocysteine beta-lyase and methylselenol demethylase in the metabolism of Se-methylated selenocompounds into selenide. *Biochim Biophys Acta*. 2007;1770(7):1053-1061. doi:10.1016/j.bbagen.2007.03.007
64. Gabel-Jensen C, Odgaard J, Skonberg C, Badolo L, Gammelgaard B. LC-ICP-MS and LC-ESI-(MS)n identification of Se-methylselenocysteine and selenomethionine as metabolites of methylseleninic acid in rat hepatocytes. 10.1039/B807805J. *Journal of Analytical Atomic Spectrometry*. 2009;24(1):69-75. doi:10.1039/B807805J
65. Dauplais M, Mahou P, Plateau P, Lazard M. Exposure to the Methylselenol Precursor Dimethyldiselenide Induces a Reductive Endoplasmic Reticulum Stress in Saccharomyces cerevisiae. *Int J Mol Sci*. 2021;22(11):5467.

Statements and Declarations

Funding: This research received no external funding.

Declaration of competing interest: The authors declare that there is no potential conflict of interests.

Author Contributions: Conceptualization, Myriam Lazard; Material preparation, data collection and analysis were performed by Marc Dauplais, Stephane Romero and Myriam Lazard. The original draft was written by Myriam Lazard and reviewed by Marc Dauplais and Stephane Romero. All authors read and approved the final version of the manuscript.

Data Availability Data will be shared upon request to the corresponding author: myriam.lazard@polytechnique.edu

Ethics approval: Not applicable

Informed Consent Statement: Not applicable